EVOLUTION & DEVELOPMENT 11:4, 441–455 (2009)
DOI: 10.1111/j.1525-142X.2009.00350.x

Post-embryonic development of the Furongian (late Cambrian) trilobite *Tsinania canens*: implications for life mode and phylogeny

Tae-yoon Park* and Duck K. Choi

School of Earth and Environmental Sciences, Seoul National University, Seoul 151-747, Korea

*Author for correspondence (email: taeyoon.park@hotmail.com)

SUMMARY The current concept of the order Asaphida was proposed to accommodate some Cambrian and Ordovician trilobite clades that are characterized by the possession of a ventral median suture. The family Tsinaniidae was recently suggested to be a member of the order Asaphida on the basis of its close morphological similarity to Asaphidae. Post-embryonic development of the tsinaniid trilobite, *Tsinania canens*, from the Furongian (late Cambrian) Hwajeol Formation of Korea, reveals that this trilobite had an adult-like protaspis. Notable morphological changes with growth comprise the effacement of dorsal furrows, sudden degeneration of pygidial spines, regression of genal spines, and loss of a triangular rostral plate to form a ventral median suture. Programmed cell death may be responsible for degenerating the pygidial and genal spines during ontogeny. Morphological changes with growth, such as the loss of pygidial spines, modification of pleural tips, and effacement of dorsal furrows, suggest that *T. canens* changed its life mode during ontogeny from benthic crawling to infaunal. The protaspid morphology and the immature morphology of *T. canens* retaining genal and pygidial spines suggest that tsinaniids bear a close affinity to leiostegioids of the order Corynexochida. Accordingly, development of a ventral median suture in *T. canens* demonstrates that the ventral median suture could have evolved polyphyletically, and thus the current concept of the order Asaphida needs to be revised.

INTRODUCTION

The Paleozoic arthropod group, Trilobita, left a rich fossil record and is one of the most intensively studied fossil groups during the past two centuries. Nevertheless, its phylogeny has still remained poorly resolved due mainly to our incomplete understanding of the Cambrian origin of the post-Cambrian trilobite clades (Fortey 2001; Whittington 2007). Larval morphology is generally regarded to be informative and useful for resolving the higher-level classification of trilobites (Whittington 1957, 2007; Chatterton and Speyer 1997; Fortey 2001). It has been widely used in trilobite taxonomy (e.g., Fortey and Owens 1975; Chatterton 1980; Chatterton et al. 1994; Lee and Chatterton 2003) and is also expected to play a vital role in elucidating the Cambrian trilobite phylogeny (Fortey 2001; Whittington 2007).

Fortey and Chatterton (1988) and Fortey (1990) emended the order Asaphida to accommodate several Cambrian and Ordovician clades, which are characterized by a globular larva, called an "asaphoid protaspis," and a ventral median suture. The ventral median suture was considered as the key synapomorphy of the order Asaphida, whereas the asaphoid protaspis was regarded as the synapomorphy of less inclusive group within the order (Fortey and Chatterton 1988, text-fig. 1). The concept of the order Asaphida has stood the test of time for the past 20 years and has been increasingly used in trilobite classification.

The late Cambrian (Furongian) trilobite family Tsinaniidae was assigned to Asaphoidea by Hupé (1955), but Shergold (1975, 1991) considered it as a member of Leiostegioidea that belongs to the order Corynexochida. Fortey (1990, p. 564) suggested that this family may provide evidence of leiostegioidean ancestry of Illaenoidea, and later placed Tsinaniidae in the Superfamily Illaenoidea, which also belongs to the order Corynexochida (Fortey 1997). Recently, Zhu et al. (2007) assigned Tsinaniidae to the order Asaphida, based on the morphological features shared by the tsinaniid trilobite, *Shergoldia laevigata* Zhu et al. (2007), and asaphid trilobites: that is, conterminant hypostomal condition, eight homonomous thoracic segments in the holaspid phase, isolated form of the S1 furrows, bacculae, eye socles, and no circumocular suture.

This study explores the post-embryonic development of the Furongian tsinaniid trilobite, *Tsinania canens* (Walcott 1905), based on silicified sclerites from Korea. *T. canens* and *S. laevigata* reveal their close relationship in sharing morphological features such as the effaced surface, isopygous pygidium, and supramarginal anterior branches of the facial suture. Moreover, the two trilobites display similar morphological changes during growth including the sudden degeneration of pygidial spines and the regression of the genal spines.

It is expected that the larval morphology of *T. canens* will help determine the systematic position of the Tsinaniidae among the major trilobite clades. In addition, the ontogenetic information of *T. canens* will be beneficial for elucidating the phylogenetic relationships of Cambrian trilobites.

FOSSIL LOCALITY, MATERIAL, AND METHODS

All of the specimens considered in this study were collected from the lowermost part of the Hwajeol Formation in the Sagundari section (37°04′57″N, 129°01′03″E) in the Taebaeksan Basin, central-eastern part of the Korean peninsula (see Sohn and Choi 2007). The Hwajeol Formation consists mainly of alternating limestone and shale beds, with frequent intercalation of limestone conglomerate beds (Choi et al. 2004), and is thought to have been deposited in inner to outer ramp environments (Kwon et al. 2006). The lowermost part of the Hwajeol Formation at the Sagundari section comprises a limestone–shale couplet facies, from which Sohn and Choi (2007) recently recorded the following trilobites: *Pseudagnostus planulatus*, *Asioptychaspis subglobosa*, *Haniwa sosanensis*, and *T. canens*. They demonstrated that the lowermost part of the formation represents the *Asioptychaspis* Zone, which is middle Furongian in age. Fossil-bearing limestone–shale couplet samples from the horizon 2.5 m above the base of the formation were digested with 7% hydrochloric acid. Numerous silicified trilobite sclerites were recovered from the residues. Specimens of *T. canens* are invariably disarticulated. A total of 915 specimens of *T. canens* including 123 protaspides, 290 cranidia, 122 free cheeks, 54 thoracic segments, and 326 pygidia were isolated. All illustrated specimens are deposited in the paleontological collections of Seoul National University with registered SNUP numbers.

To visualize the change in the length of the genal and pygidial spines with growth, the centroid size of the free cheeks and the pygidia was calculated. Centroid size is the square root of the sum of squared distances of all landmarks from the centroid of the landmarks (Bookstein 1991). Ten landmarks were selected for free cheeks and six geometric points for pygidia (Fig. 1). As the pygidium underwent a dynamic morphologic change during the meraspid phase during which new segments proliferated at the rear end and the anteriormost segment of pygidium was released into the thorax at each molt, the six geometric points of each meraspid degree are not homologous with those of other meraspid degrees, and hence cannot be referred to strictly as landmarks with respect to segment identity (see Zelditch et al. 2004 for a definition of landmarks). Nevertheless, we used the six geometric points to obtain the centroid size of each pygidium in order to acquire a reliable proxy for overall size. Landmarks or geometric points of each specimen were marked using the program tpsDig 2, whereas CoordGen 6.0 was used to compute the centroid size. The tpsDig 2 was developed by F. J. Rohlf (http://life.bio.sunysb.edu/morph/) and CoordGen 6.0 was created by D. Sheets (http://www.canisius.edu/ ~ sheets/morphsoft.html): both programs are freely available online.

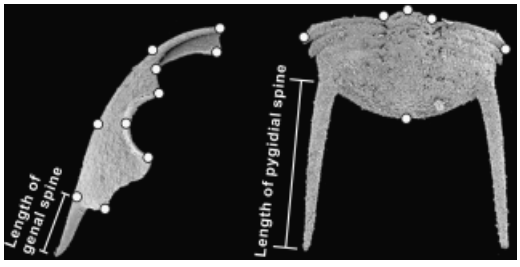

Fig. 1. Position of landmarks on free cheek and geometric points on pygidium of *Tsinania canens*, selected for computing centroid size.

ONTOGENY OF *T. CANENS*

Trilobite ontogeny has been comprehensively reviewed by Chatterton and Speyer (1997) and Hughes et al. (2006). The embryonic stages of trilobites are not known. Traditionally, post-embryonic development of trilobites has been divided into three phases in terms of trunk articulation: protaspid, meraspid, and holaspid phases. The protaspid phase is characterized by having trunk segments fused to the cephalon. The meraspid phase began when the first articulation appeared between the cephalon and the trunk. During this phase, thoracic segments were released from the anteriormost end of the meraspid pygidium, whereas new segments are generated at the terminal growth zone of the meraspid pygidium. The number of the thoracic segments defines the degree of the meraspid stages. The holaspid phase commenced when the last thoracic segment was released, and hence no increase of thoracic segments in subsequent molting. In addition, Hughes et al. (2006) suggested a division of trilobite ontogeny into two phases with respect to segment generation: the anamorphic phase during which new trunk segments appeared, and the subsequent epimorphic phase, during which the number of segments in the trunk no longer increased. Zhu et al. (2007) noted that the mode of trunk development in tsinaniids was protarthrous, based on the fact that onset of the holaspid phase precedes onset of the epimorphic phase in *S. laevigata*. This study, however, does not consider the ontogeny of *T. canens* with respect to segment generation, as the highly effaced exoskeleton of *T. canens* hinders accurate determination of the segment numbers.

Protaspid phase

The protaspides of *T. canens* can be differentiated into the early and late stages by size and morphology. They form two distinct clusters in the bivariate plots of exoskeletal length versus width (Fig. 2).

The early stage protaspides (Fig. 3, A–P) are circular in outline, 0.33–0.52 mm long and 0.32–0.57 mm wide, and moderately globular in lateral view. The lateral margin is

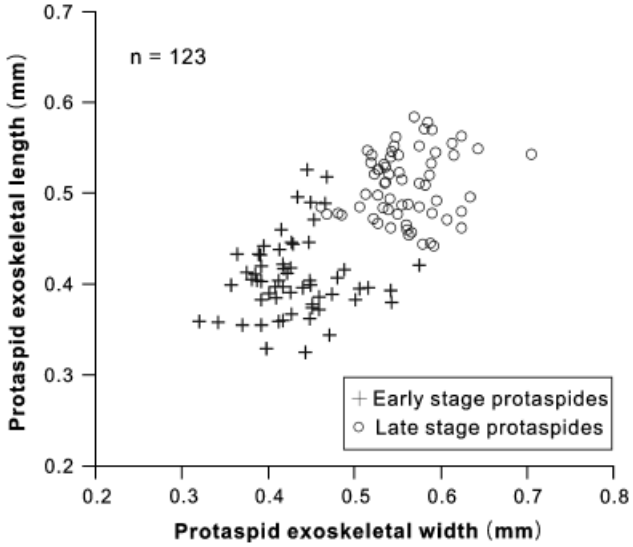

Fig. 2. Scatter plots of length versus width for protaspid exoskeletons of *Tsinania canens*.

sinuous, representing the location of the facial suture; axial furrows are shallow, impressed only in the frontal half of exoskeleton; the glabella slightly expands forward with a pair of anterior pits; and a pair of spines are present on the posterior margin of the exoskeleton.

The late stage protaspides (Fig. 3, Q–Z) are subhexagonal in outline, 0.44–0.58 mm long and 0.46–0.70 mm wide. The glabella is subparallel to slightly expanding forward, well defined by axial furrows; anterior pits are moderately impressed; palpebral lobes are short and narrow, situated in front of glabellar midlength; occipital furrow is shallow; posterior border furrow is clearly incised; posterior cranidial marginal furrows are transverse and moderately deep; the trunk is inverted trapezoidal in outline, 19–30% of sagittal exoskeletal length, strongly downsloping posteriorly; and the lateral margin of protopygidium is slightly upturned.

Post-protaspid cranidia

Five developmental stages have been recognized for the post-protaspid cranidia of *T. canens* according to morphologic changes with growth (Fig. 4). No attempt has been made to differentiate the meraspid and holaspid phases.

The developmental stage 1 cranidia (Fig. 5, A–D) are 0.40–0.60 mm long and 0.56–0.84 mm wide, subtrapezoidal in outline, with subparallel, well defined axial furrows. The posterior cranidial border widens abaxially, defined by deep posterior border furrows. The low variation in morphology and close clustering in the bivariate plots (Fig. 4) suggests that this phase may represent the first meraspid instar.

The developmental stage 2 cranidia (Fig. 5, E–J) are 0.52–1.05 mm long and 0.97–1.80 mm wide. This developmental stage is defined by the appearance of a short anterior cranidial border. The outline of the cranidium is more transverse and the palpebral lobes are longer than those of developmental

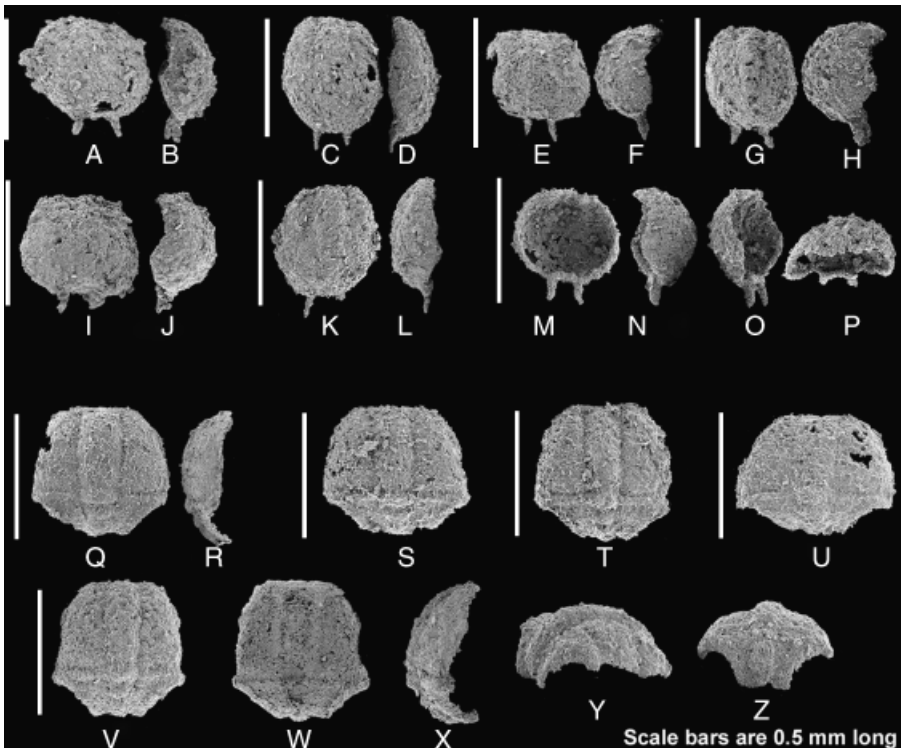

Fig. 3. Protaspides of *Tsinania canens* (Walcott 1905). A–P, early stage protaspides. A, B, SNUP4753; A, dorsal and B, lateral views. C, D, SNUP4754; C, dorsal and D, lateral views. E, F, SNUP4755; E, dorsal and F, lateral views. G, H, SNUP4756; G, dorsal and H, lateral views. I, J, SNUP4757; I, dorsal and J, lateral views. K, L, SNUP4758; K, dorsal and L, lateral views. M–P, SNUP4759; M, ventral, N, lateral, O, ventro-lateral, and P, antero-ventral views. Q–Z, late stage protaspides. Q, R, SNUP4760; Q, dorsal, and R, lateral views. S, dorsal view, SNUP4761. T, dorsal view, SNUP4762. U, dorsal view, SNUP4763. V–Z, SNUP4764; V, dorsal, W, ventral, X, lateral, Y, posterolateral, and Z, posterior views.

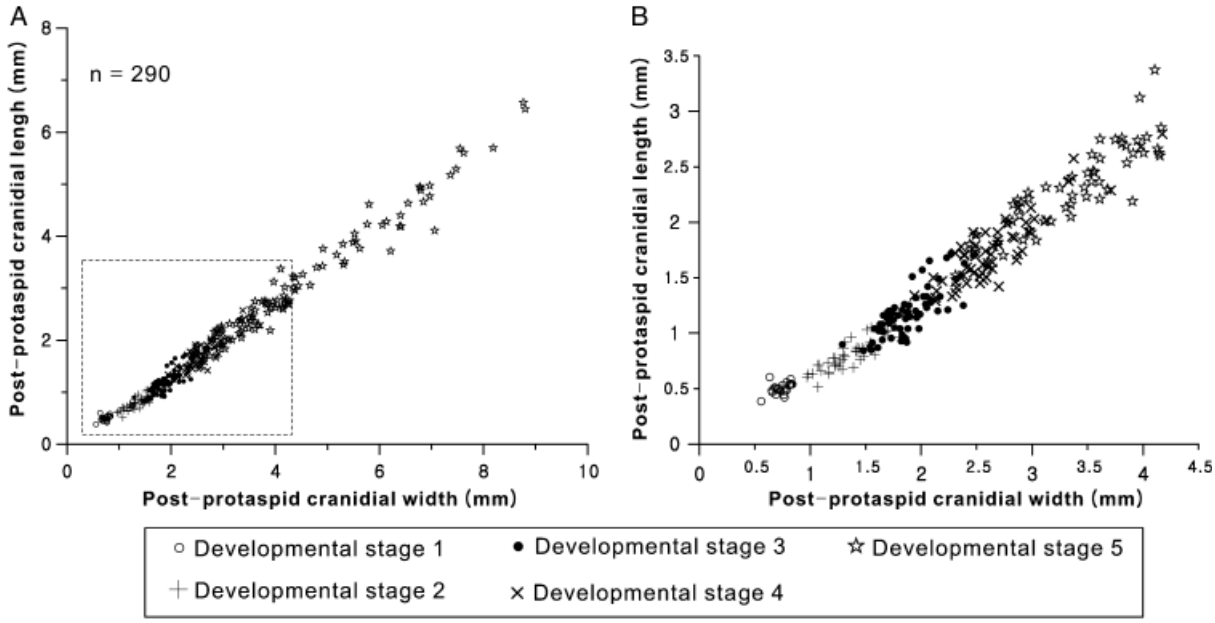

Fig. 4. Scatter plots of length versus width for post-protaspid cranidia of *T. canens*. The dotted rectangle in (A) denotes the portion which is magnified in (B).

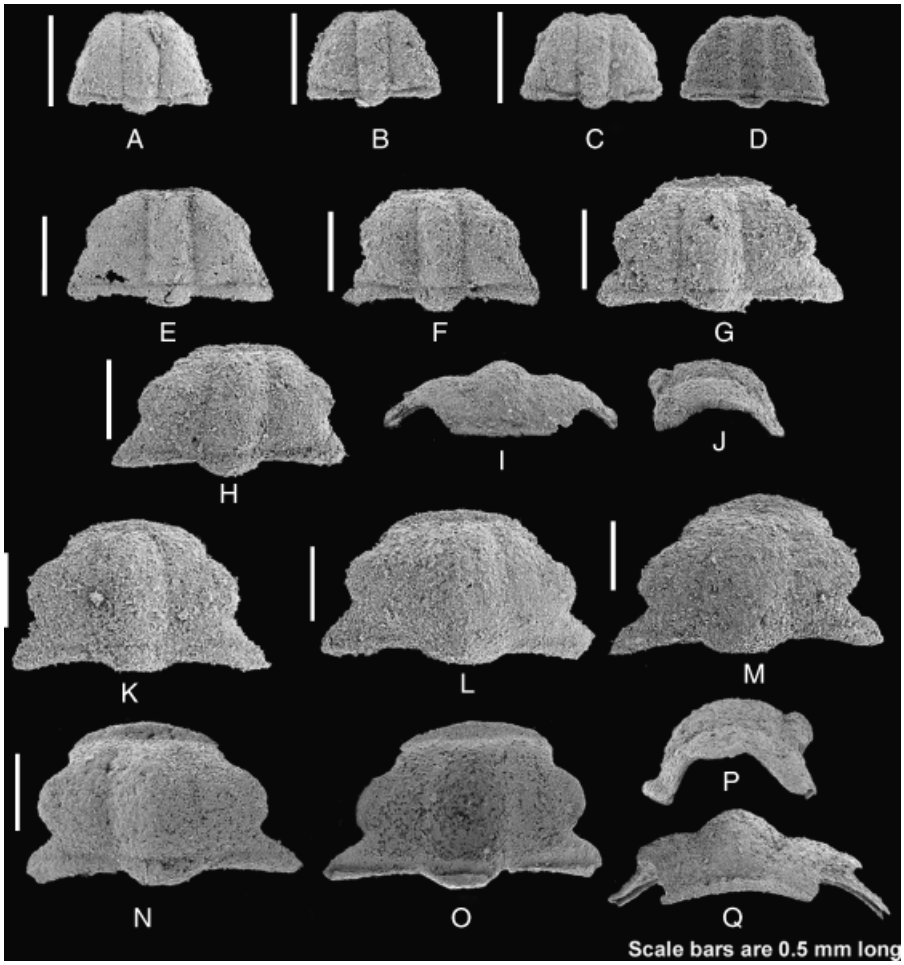

Fig. 5. Post-protaspid cranidia of *Tsinania canens* in the developmental stages 1–3. A–D, cranidia in the developmental stage 1. A, dorsal view, SNUP4765. B, dorsal view, SNUP4766. C, D, SNUP4767; C, dorsal and D, ventral views. E–J, cranidia in the developmental stage 2. E, dorsal view, SNUP4768. F, dorsal view, SNUP4769. G, dorsal view, SNUP4770. H–I, SNUP4771; H, dorsal, I, anterior, and J, lateral views. K–Q, cranidia in the developmental stage 3. K, dorsal view, SNUP4772. L, dorsal view, SNUP4773. M, dorsal view, SNUP4774. N–Q, SNUP4775; N, dorsal, O, ventral, P, lateral, and Q, anterior views.

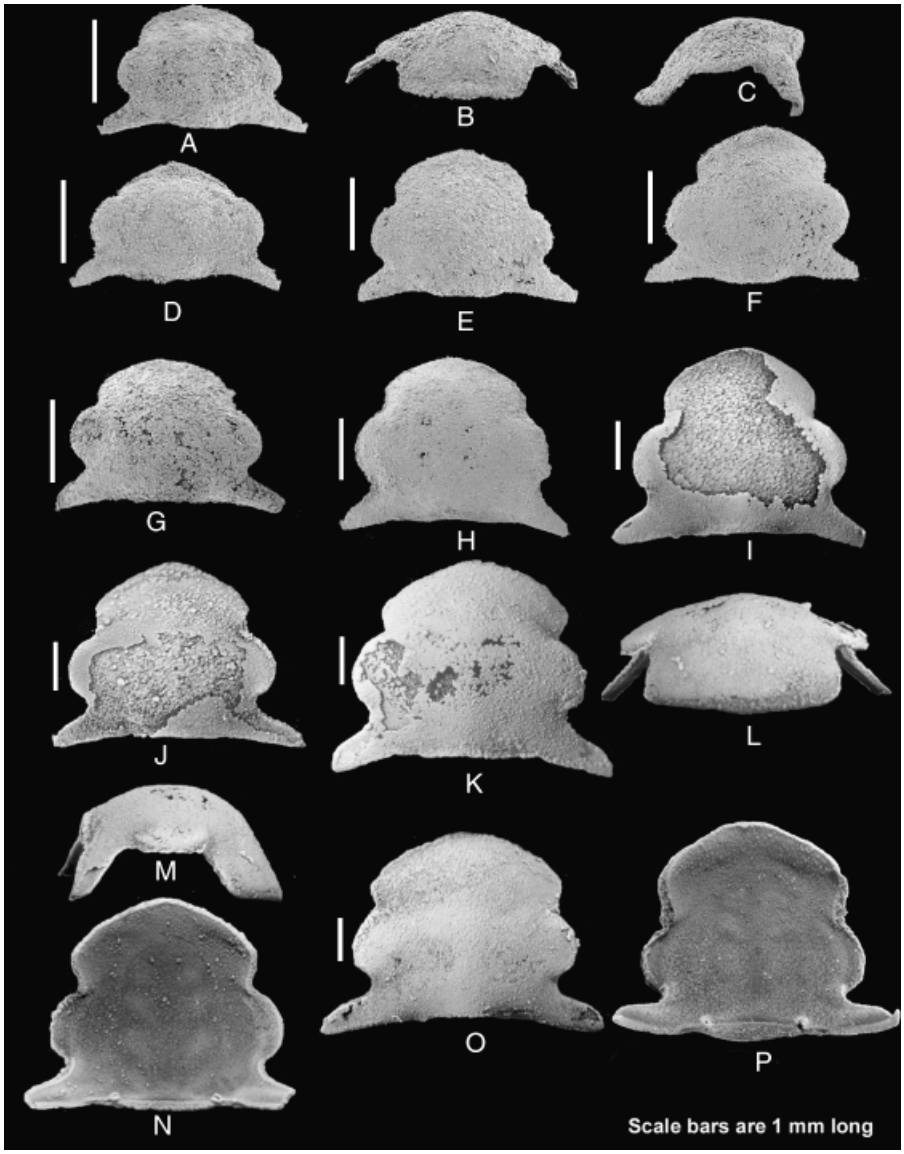

Fig. 6. Post-protaspid cranidia of *Tsinania canens* in the developmental stages 4 and 5. A–F, craidia in the developmental stage 4. A–C, SNUP4776; A, dorsal, B, anterior, and C, lateral views. D, dorsal view, SNUP4777. E, dorsal view, SNUP4778. F, dorsal view, SNUP4779. G–O, cranidia in the developmental stage 5. G, dorsal view, SNUP4780. H, dorsal view, SNUP4781. I, dorsal view, SNUP4782. J, dorsal view, SNUP4783. K–N, SNUP4784; K, dorsal, L, anterior, M, lateral, and N, ventral views. O, P, SNUP4785; O, dorsal and P, ventral views.

stage 1. The posterolateral projections of the fixigenae appear to be better developed.

The developmental stage 3 cranidia (Fig. 5, K–Q) are 0.84–1.72 mm long and 1.29–2.47 mm wide. Compared with the previous stage, the cranidia are more convex; the anterior cranidial border is longer; the glabella is broader; and the dorsal furrows become more effaced. The palpebral lobes are about one-third of the cranidial length, situated at the glabellar midlength. The anterior cranidial border is weakly convex forward.

The developmental stage 4 cranidia (Fig. 6, A–F) are 1.18–2.80 mm long and 1.85–4.17 mm wide. The anterior cranidial border furrow is faintly indicated, whereas other furrows are effaced. The anterior margin is weakly angulated. The occipital ring is comparatively shorter than that of the previous stage.

The developmental stage 5 cranidia (Fig. 6, G–P) have no dorsal furrows on the surface. The smallest cranidium is 1.52 mm long and 2.31 mm wide. Pairs of muscle scar-like impressions are visible on the ventral surface of the glabella (Fig. 6, N and P). The short doublure of the occipital ring is flanked by downwardly directed ball-like structures (Fig. 6, N and O).

Free cheeks

Small free cheeks that may match developmental stages 1 and 2 cranidia have not been recovered. The morphological

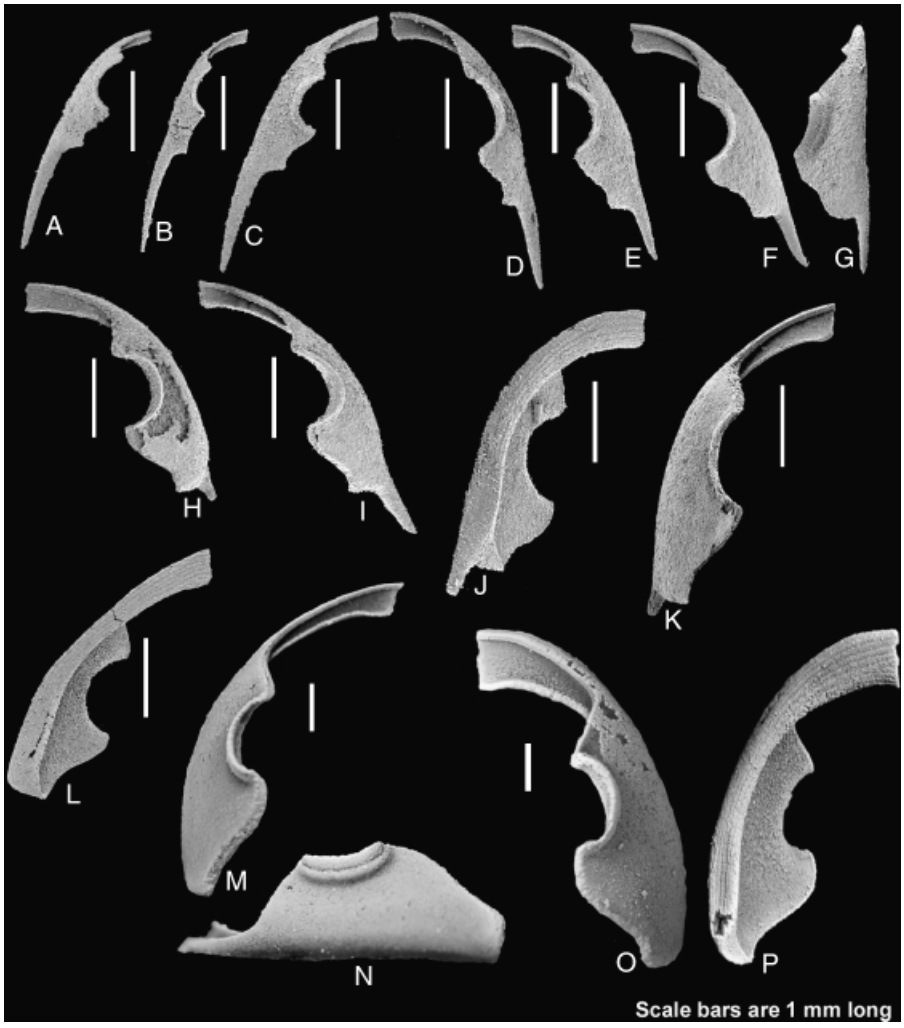

Fig. 7. Free cheeks of *Tsinania canens*. A, dorsal view, SNUP4786. B, dorsal view, SNUP4787. C, dorsal view, SNUP4788. D, dorsal view, SNUP4789. E, dorsal view, SNUP4790. F, G, SNUP4791; F, dorsal and G, lateral view. H, dorsal view, SNUP4792. I, dorsal view, SNUP4793. J, ventral view, SNUP4794. K, dorsal view, SNUP4795. L, ventral view, SNUP4796. M, N, SNUP4797; M, dorsal and N, lateral views. O, P, SNUP4798; O, dorsal and P, ventral views. Note the visual surfaces are recognizable in G and N.

features of free cheeks of *T. canens* include an effaced surface, narrow eye socle, visual surface fused to an eye socle, and terrace lines on the doublure (Fig. 7). The adaxial tip of the cephalic doublure indicates that, when fully articulated, a small triangular rostral plate would have existed behind a ventral median suture as in *S. laevigata* (Zhu et al. 2007). However, the largest free cheek (Fig. 7, O and P) shows no place for a rostral plate, which implies that the rostral plate would have disappeared with growth, forming a ventral median suture. The reduction of the triangular rostral plate during growth is also recognizable in specimens of *S. laevigata* illustrated in Zhu et al. (2007, Fig. 3): the smallest specimen has a relatively large rostral plate, whereas the large specimens bear smaller rostral plates. The reduction of the rostral plate during growth in both *Tsinania* and *Shergoldia* also corroborates their close phylogenetic relationship.

Small free cheeks (Fig. 7, A and B) bear a genal spine that is almost as long as the genal field. With growth, the genal spine shortened such that specimens of intermediate size have short spines (Fig. 7, H, J, K), and eventually the genal spine completely disappeared in large specimens (Fig. 7, L–P). The regression of the genal spine is well represented in the bivariate plots of the length of the genal spine versus the centroid size (Fig. 8).

Thoracic segments

Considering the size, all disarticulated thoracic segments of *T. canens* observed in this study (Fig. 9) likely represent postmeraspid stages. Morphological features of the thoracic segments include the anteriorly pointed lateral tip of the pleura, an articulating facet on the anterolateral margin, a short articulating half-ring, paired protuberances at the posterior end of the ventral surface of the axis, a panderian notch, and a panderian protuberance.

The ventral protuberances in the posterior end of axis would have been used as the ball-and-socket joints as in the case of the illaenid trilobite, *Bumastoides lenzi* Chatterton

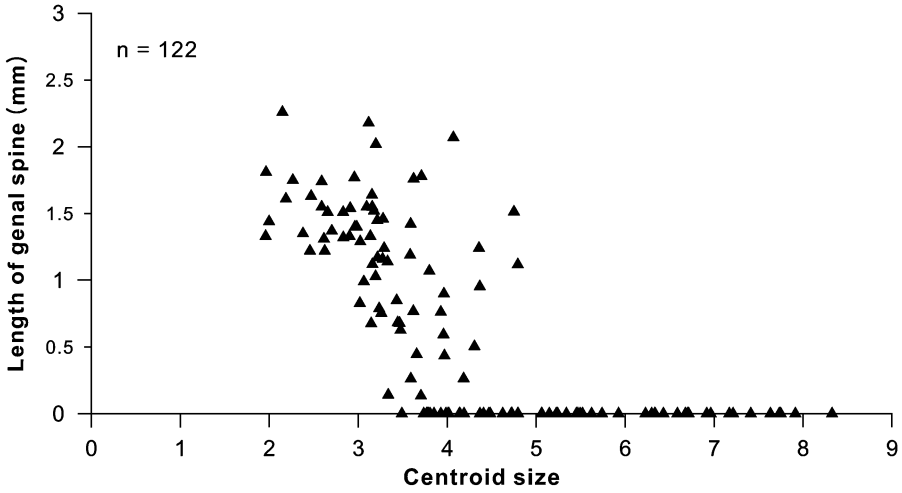

Fig. 8. Centroid size of free cheeks of *Tsinania canens* as a function of the length of genal spine. Note that as the size of free cheek increases, the genal spine progressively regresses.

and Ludvigsen (1976), demonstrated by Westrop (1983). These structures are comparable to the protuberances at the posterior end of the ventral side of large cranidia (Fig. 6, N and P). The panderian protuberance at the anterior margin of the pleural doublure is clearly seen in the posterior view (Fig. 9, D, F, and J).

Post-protaspid pygidia

For pygidia, it is possible to recognize the meraspid stages and the entry into the holaspid phase by observing the relative position of the pygidial spine-bearing segment (PSS) that is destined to be the anterior-most segment in the holaspid pygidia. Because the number of thoracic segments of *T. canens* is not known, in order to indicate the developmental stages of meraspid pygidia, we will use the "PSS+*n*" scheme in which "*n*" denotes the number of segments in front of the PSS in the meraspid pygidium. For instance, the PSS+1 stage refers to the meraspid degree in which the number of the thoracic segments is one less than that of holaspis. However, counting the number of segments in front of the PSS is not possible for the small pygidia in which the PSS has yet to appear and for those in which the number of segments in front of the PSS is indeterminable. These small meraspid pygidia are divided into three stages according to morphology and size: the early developmental stages 1–3. Subsequent meraspid stages can be divided into five stages: from the PSS+5 to PSS+1 stages. The holaspid phase is divided into two stages: the early stage retaining a pair of pygidial spines and the late stage without the pygidial spines. Accordingly, the post-protaspid pygidial development of *T. canens* is differentiated into 10 developmental stages (Fig. 10).

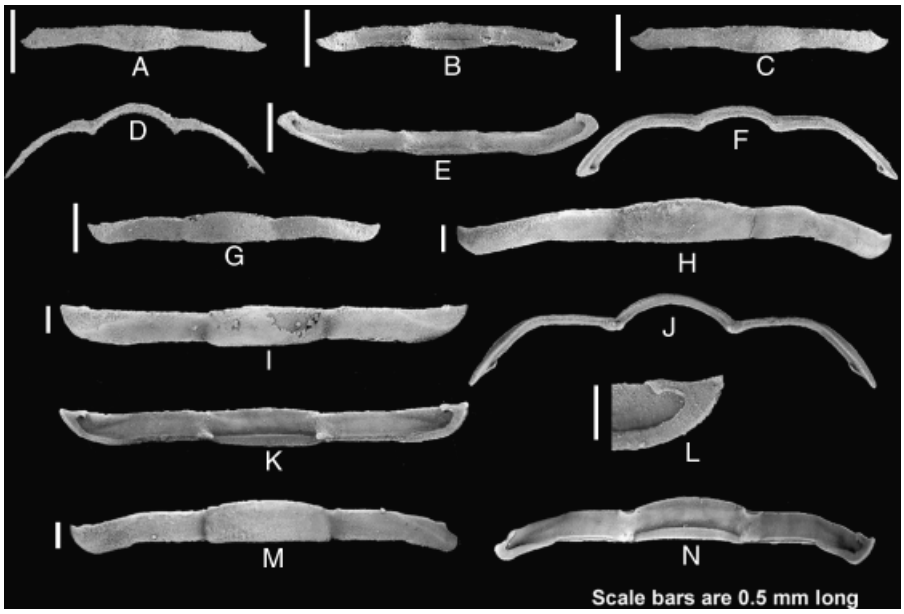

Fig. 9. Thoracic segments of *Tsinania canens*. A, dorsal view, SNUP4800. B, ventral view, SNUP4801. C, D, SNUP4802; C, dorsal and D, posterior views. E, F, SNUP4803; E, ventral and F, posterior views. G, dorsal view, SNUP4804. H, dorsal view, SNUP4805. I–L, SNUP4806; I, dorsal, J, posterior, and K, ventral views. L, close up of the ventral doublure; note the panderian protuberance and the panderian notch. M, N, SNUP4807; M, dorsal and N, ventral views. Note the faint transverse ventral ridge indicated by white arrow.

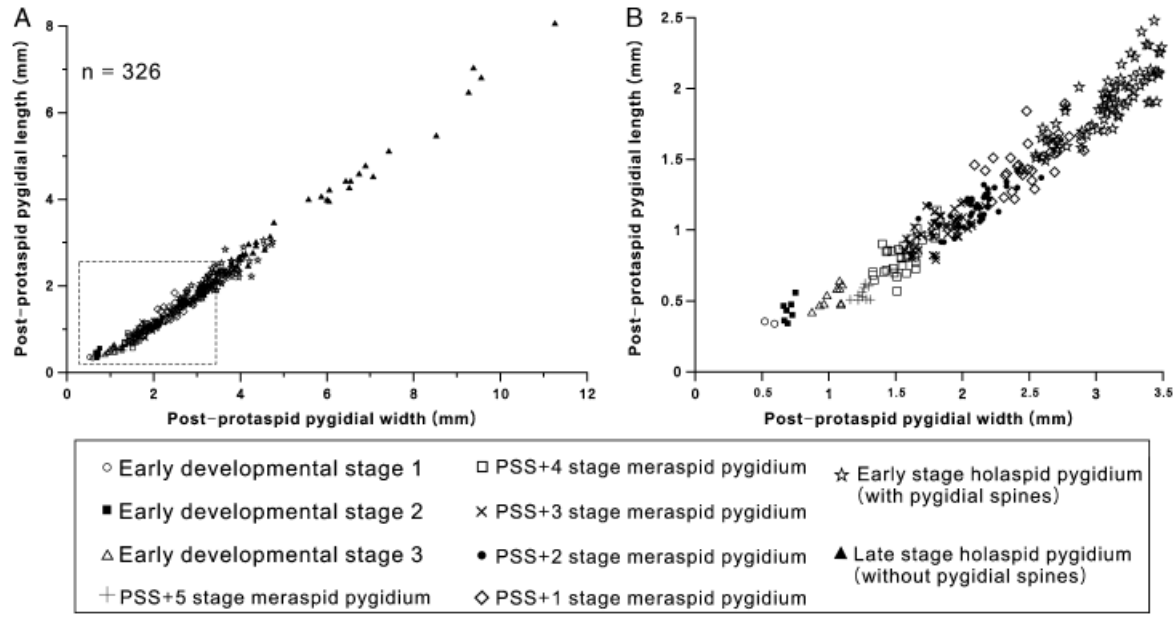

Fig. 10. Scatter plots of length versus width for post-protaspid pygidia of *Tsinania canens*. The dotted rectangle in (A) denotes the portion which is magnified in (B).

The early developmental stage 1 pygidia (Fig. 11, A and B) are inverted trapezoidal in outline with a moderately indented posterior margin. The lateral margin is more upturned compared with the protopygidia of the late stage protaspides. No pygidial spines are developed in this stage, but it cannot be ruled out that the PSS may have been generated at the terminal growth zone without expressing the pygidial spines.

The early developmental stage 2 pygidia (Fig. 11, C–F) bear a pair of pygidial spines, indicating that the PSS has been clearly generated by this stage. The posteriorly directed spines are subparallel and are 0.8–1.8 times as long as the pygidium.

The early developmental stage 3 pygidia (Fig. 11, G–I) are distinguished from the previous stage in having a more transverse outline and posteriorly divergent pygidial spines. The pygidial spines form an angle of about 40°, and are 1.9–2.8 times as long as the pygidium. The posterior margin is less indented than that of developmental stage 2 pygidia, presumably due to the proliferation of new segments at the rear end of the pygidium.

The PSS+5 stage meraspid pygidia (Fig. 11, J–L) are recognized by five segments in front of the pygidial spine-bearing segment. The pygidial spines are divergent backwards, forming an angle of 50–70°, and are 2.5–2.6 times as long as the pygidium.

The PSS+4 stage meraspid pygidia (Fig. 11, M–O) have pygidial spines that are 1.6–2.7 times as long as the pygidium. The angle between the pygidial spines is 30–50°. The posterior margin is broadly rounded. The segments behind the PSS, destined to form the holaspid pygidia together with PSS, are morphologically discernable from the segments in front of the PSS in having an effaced dorsal surface.

In the PSS+3 stage meraspid pygidia (Fig. 12, A–E), the pygidial spines are 1.5–2.4 times as long as the pygidium. The angle between the pygidial spines is variable: some pygidial spines are subparallel (Fig. 12B), whereas others form an angle of ca. 50° (Fig. 12C).

In the PSS+2 stage meraspid pygidia (Fig. 12, F–K), the pygidial spines are 1.4–1.8 times as long as the pygidium. The pygidial spines are subparallel to slightly divergent backward. Pleural and interpleural furrows are weakly impressed in front of the pygidial spine-bearing segment. Terrace lines are observed on the doublure (Fig. 12G).

The PSS+1 stage meraspid pygidia (Fig. 12, L–R) have a highly effaced surface with furrows just behind the anteriormost segment. The pygidial spines are 1.2–1.6 times as long as the pygidium, and are subparallel to slightly divergent backward.

The early stage holaspid pygidia (Fig. 13, A–F) have no segments in front of the PSS. The small early stage holaspid pygidia have pygidial spines slightly divergent backwards, whereas in large early stage holaspid pygidia the pygidial spines weakly converge backwards. The largest early stage holaspid pygidium (Fig. 13F) is 3.02 mm long.

The late stage holaspid pygidia (Fig. 13, G–L) lack the pygidial spines. The sudden degeneration of the pygidial spines is well represented in the bivariate plots of the centroid size of the pygidia versus the length of the pygidial spines (Fig. 14). The smallest late stage holaspid pygidium is 2.45 mm in

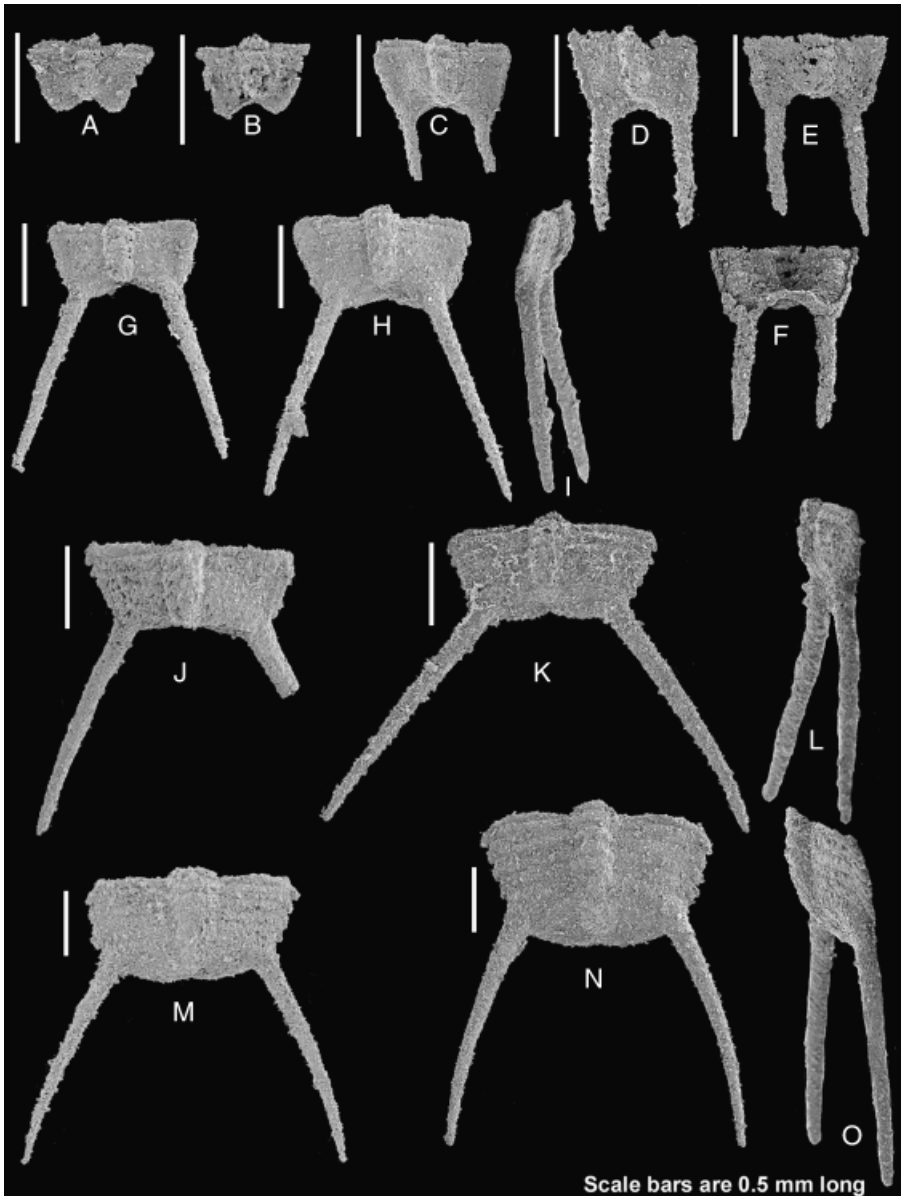

Fig. 11. Meraspid pygidia of *Tsinania canens* in the early developmental stages 1–3, pygidial spine-bearing segment (PSS)+5, and PSS+4 meraspid stages. A, B, meraspid pygidia in the early developmental stage 1. A, dorsal view, SNUP4808. B, dorsal view, SNUP4809. C–F, early developmental stage 2 pygidia. C, dorsal view, SNUP4810. D, dorsal view, SNUP4811. E, F, SNUP4812; E, dorsal and F, ventral views. G–I, early developmental stage 3 pygidia. G, dorsal view, SNUP4813. H, I, SNUP4814; H, dorsal and I, lateral views. J–L, PSS+5 stage meraspid pygidia. J, dorsal view, SNUP4815. K, L, SNUP4810; K, dorsal and L, lateral views. M–O, PSS+4 stage meraspid pygidia. M, dorsal view, SNUP4817. N, O, SNUP4818; N, dorsal and O, lateral views.

length. The surface is highly effaced, and the antero-lateral margin bears an articulating facet.

During the pygidial development of *T. canens*, the PSS, which is destined to be the anterior-most segment in the holaspid pygidium, is first recognized at the early developmental stage 2. Because new segments are generated at the terminal growth zone of the meraspid pygidium, it can be inferred that most, if not all, of the segments destined to be thoracic segments are already present near the onset of the meraspid phase (Fig. 15). More interestingly, subsequently generated segments behind the PSS, which are destined to comprise the holaspid pygidium, show a different pattern of development resulting in the highly effaced dorsal surface. The trunk of *T. canens* can, therefore, be considered as showing a two-batch condition in which the batch boundary coincides with the thoracic-pygidial divide in holaspis (Fig. 15), although the degree of heteronomy is not as profound as in the representative trilobites of the two-batch heteronomous trunk condition shown in Hughes (2007, Fig. 8).

DEGENERATION OF PYGIDIAL SPINES AND GENAL SPINES

During development, the genal spines and the pygidial spines of *T. canens* degenerate. It is especially notable that the loss of

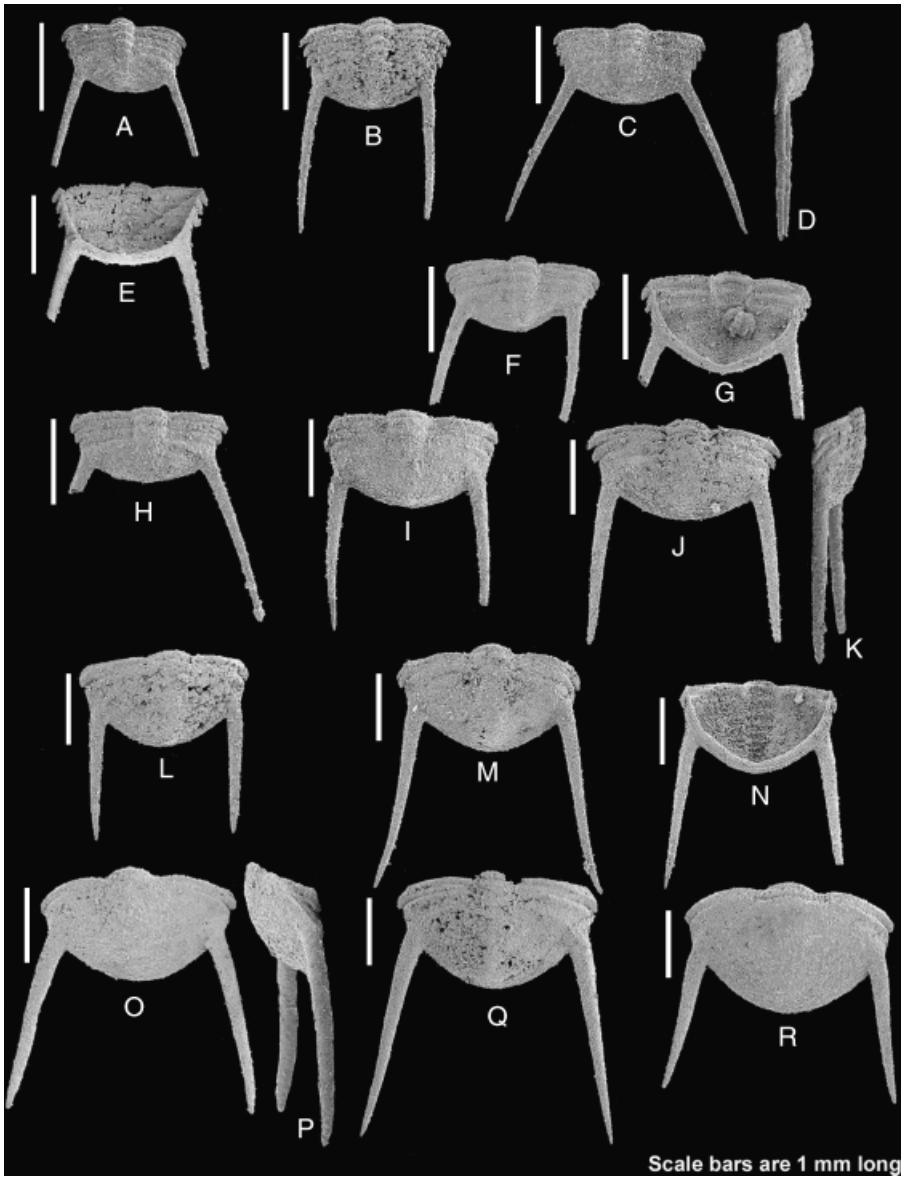

Fig. 12. Meraspid pygidia of *Tsinania canens* in pygidial spine-bearing segment (PSS)+3, 2, and 1 stages. A–E, PSS+3 stage meraspid pygidia. A, dorsal view, SNUP4819. B, dorsal views, SNUP4820. C, D, SNUP4821; C, dorsal and D, lateral views. E, ventral view, SNUP4822. F–K, PSS+2 stage meraspid pygidia. F, dorsal view, SNUP4823. G, ventral view, SNUP4824. H, dorsal view, SNUP4825. I, dorsal view, SNUP4826. J, K, SNUP4827; J, dorsal and K, lateral views. L–R, PSS+1 stage meraspid pygidia. L, dorsal view, SNUP4828. M, dorsal view, SNUP4829. N, ventral view, SNUP4830. O, P, SNUP4831; O, dorsal and P, lateral views. Q, dorsal view, SNUP4832. R, dorsal view, SNUP4833.

those structures occurred at a somewhat late stage of development. Degeneration of spine-like structures during the holaspid phase is an extraordinary phenomenon in trilobite development and has rarely been reported.

Programmed cell death (PCD) plays a critical role in all metazoan development, of which the underlying mechanism is usually conserved (Jacobson et al. 1997; Milligan and Schwartz 1997; Vaux and Korsmeyer 1999). To remove unwanted cells, PCD sculpts various body structures, deletes unneeded structures and cells, controls cell numbers, and produces differentiated cells without organelles (reviewed in Jacobson et al. 1997). Eliminating transitory structures during development is a phenomenon resulting from PCD. For example, PCD is involved in the degeneration of an amphibian tail (Tata 1966; Nakajima et al. 2005), the embryonic tail of humans (Fallon and Simandl 1978; Sapunar et al. 2001), and intersegmental muscles of a moth (Schwartz 1992) and a fly (Kimura and Truman 1990).

The progressive reduction of the genal spines of *T. canens* (Figs. 7 and 8) is superficially comparable to that of an amphibian tail (see Nakajima et al. 2005), and may be attributable to programmed cell death. On the other hand, sudden removal of an entire structure during the late stages of animal development is not a usual phenomenon in arthropods. A noticeable case would be the sudden resorption of pupal pronotal horns of the beetle *Onthophagus* (Moczek 2006; Moczek

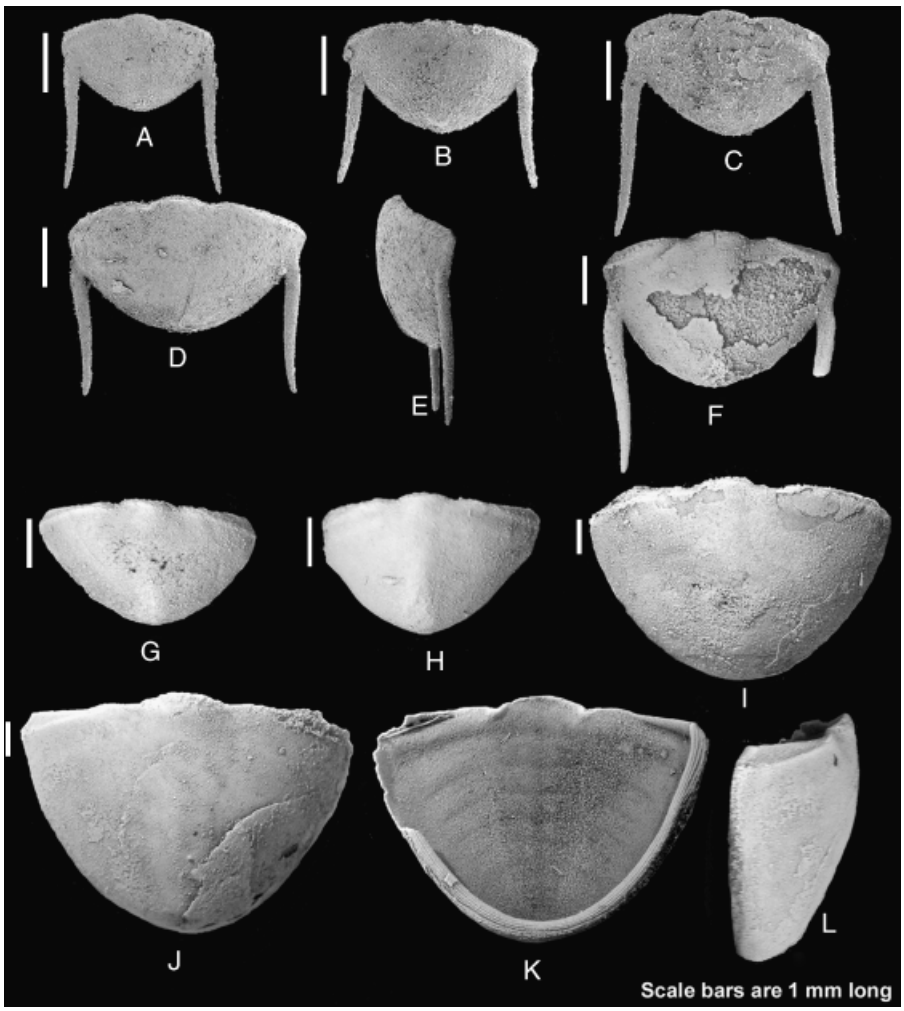

Fig. 13. Holaspid pygidia of *Tsinania canens*. A–F, early holaspid stage pygidia with pygidial spines. A, dorsal view, SNUP4834. B, dorsal view, SNUP4835. C, dorsal view, SNUP4836. D, E, SNUP4837; D, dorsal and E, lateral views. F, dorsal view, SNUP4838. G–L, late stage holaspid pygidia without pygidial spines. G, dorsal view, SNUP4839. H, dorsal view, SNUP4840. I, dorsal view, SNUP4841. J–L, SNUP4842; J, dorsal, K, ventral, and L, lateral views.

et al. 2006). Given the fact that there is no sign of shortening of the pygidial spine during the development of *T. canens* (Fig. 14), the sudden degeneration of the pygidial spines during the holaspid phase must have been achieved between adjacent molt stages: that is, in order to eliminate the pygidial spines in the subsequent instar, a massive PCD must have occurred in the epidermis before and/or immediately after molting. Such an abrupt loss of pygidial spines has not been reported in other trilobites apart from the tsinaniid trilobite *S. laevigata* (Zhu et al. 2007). Zhang and Jell (1987) considered a small pygidium of *T. canens* with pygidial spines as an immature pygidium, whereas Kobayashi (1952) misinterpreted this phenomenon in *Tsinania humilis* as "gradual disappearance of the paired spines." The radical elimination of the pygidial spines in *T. canens* must have entailed a tremendous cell death in a short period of time, which must not have been always successful: of six teratological holaspid pygidia with pygidial spines (Fig. 16), five show abnormalities in the morphology of pygidial spines (Fig. 16, B–I).

IMPLICATION FOR CHANGE IN LIFE MODE

The post-embryonic development of *T. canens* demonstrates that the exoskeletal surface of the cranidium and the pygidium became effaced with growth and both genal spines and pygidial spines were degenerated during the holaspid phase, thereby attaining a typical "illaenimorph" body plan, which is characterized by the strongly convex, effaced morphology (Westrop 1983). Illaenimorph trilobites have been considered as having an infaunal life mode in which they lived partly in a burrow (Bergström 1973; Stitt 1976; Westrop 1983). To hide the posterior part of the body into the sediment, the animals must have burrowed backwards into the sediment (Bergström 1973, p. 44), and any posteriorly directed pygidial spines would have been a hindrance for such backward movement. The pygidial spines of *T. canens* must have been functional in the early stages of development because the length of the pygidial spines kept increasing rather than degenerating before disappearing (Fig. 14). The abrupt

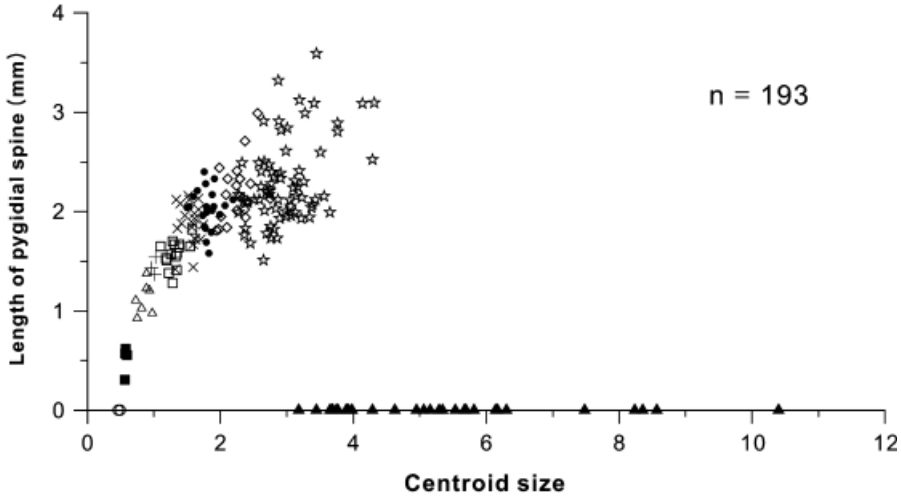

Fig. 14. Centroid size of post-protaspid pygidia of *Tsinania canens* as a function of the length of pygidial spine. A total of 160 immature pygidia retaining at least one of the pygidial spines intact were measured. Symbols are the same as in Fig. 10. Note the sudden disappearance of the pygidial spine during the holaspid phase.

loss of pygidial spines during the holaspid phase of *T. canens*, therefore, probably accompanied a change in life mode from benthic crawling to infaunal.

This change in life mode during the middle of the holaspid phase is also consistent with the morphologic change of thoracic segments during ontogeny. Even though the thoracic segments small enough to belong to the meraspid or early holaspid phase are not available in the present collection, the morphology of smaller thoracic segments can be inferred from the anterior-most segments of meraspid pygidia that are destined to be released into the thorax with subsequent development. The morphology of the anterior-most segment in the meraspid pygidia (Figs. 11 and 12) differs from that of larger holaspid thoracic segments: the lateral tips of pleurae point backward in the anterior-most segment of meraspid pygidia, whereas those of large holaspid thoracic segments point forward, and have a rounded posterolateral margin (Fig. 9). This change in the morphology of the thoracic segments may reflect a change in the life mode. The rounded posterolateral margin of the distal part of pleurae must have helped the burrowing backward movement of the animal. Had the pleural tips been backwardly directed as in the meraspid (and presumably early holaspid) thoracic segments, it would have caused extra-resistance when burrowing backwards. It is significant that two novel morphologic changes (one in thoracic segments and the other in pygidia) occurred nearly simultaneously during the holaspid phase. Taken together, it can be concluded that the ontogeny of *T. canens* demonstrates how a new morphotype for infaunal life mode evolved from the plesiomorphic morphology for benthic of a crawling life mode.

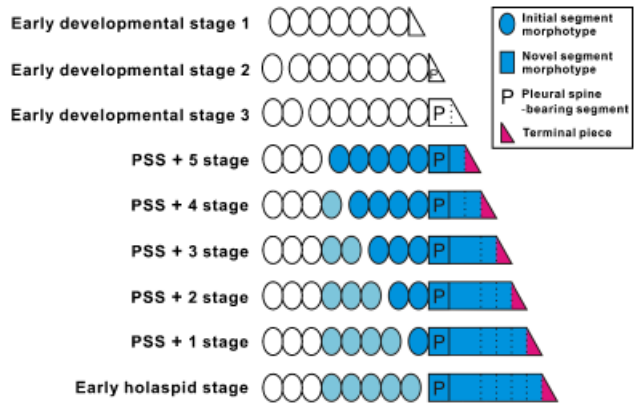

Fig. 15. Trunk segmentation schedule for *Tsinania canens*. Segments in light blue are thoracic, those in dark blue are pygidial, and the terminal piece is in red. Those not colored are the segments drawn by inference. The diagram was drawn on the basis of the assumption that one segment was released from the anterior part of the meraspid pygidium into the thorax between each stage (however, the eight thoracic segments in the holaspid phase are also known in *Shergoldia laevigata*, a close relative of *T. canens*). The exact number of pygidial segments is not known, but the dotted lines imply the generation of new segments at the terminal growth zone. Note that the pygidial spine-bearing segment marks the boundary of the two different morphological batches of trunk segments.

DISCUSSION

Suprafamilial assignment of Tsinaniidae

Fortey and Chatterton (1988) defined the "asaphoid" protaspides for those displaying a spherical to ovoid shape, with enrolled rather than inturned doublure, which subsequently metamorphosed into benthic meraspides. They stressed the asaphoid protaspis as the key feature of the derived families of order Asaphida. The late protaspis of *T. canens* is of a benthic adult-like morphology and hence is readily distinguished from the typical asaphoid protaspides. This fact casts doubt on Zhu

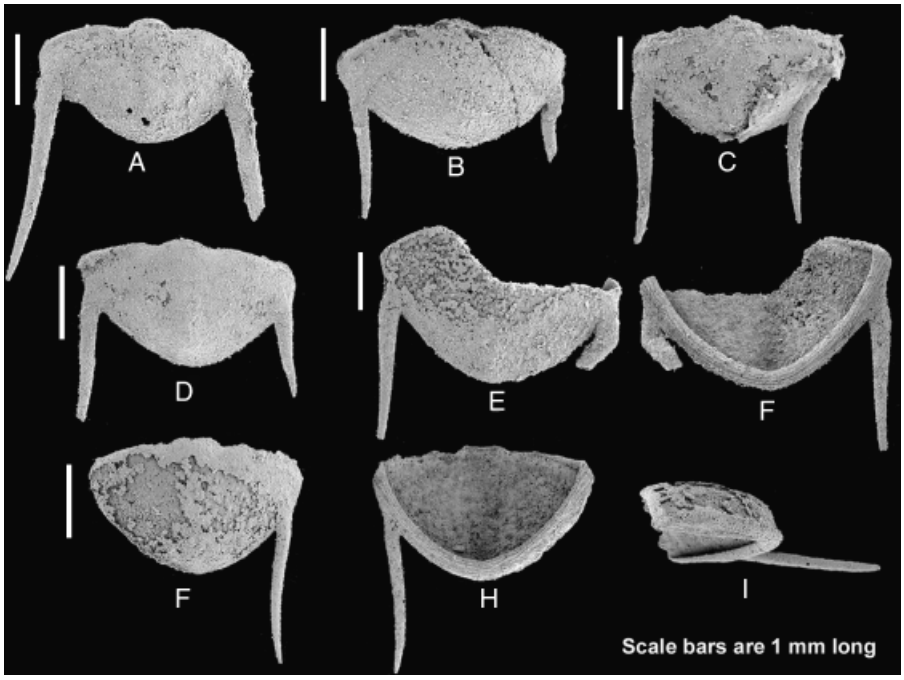

Fig. 16. Early stage holaspid pygidia with abnormality. A, dorsal view, SNUP4843. B, dorsal view, SNUP4844. C, dorsal view, SNUP4845. D, dorsal view, SNUP4846. E, F, SNUP4847; E, dorsal and F, ventral views. G–I, SNUP4848; G, dorsal, H, ventral, and I, ventro-lateral views. Note that SNUP4843 (A) shows abnormality in the posterior margin, whereas others (B–I) have abnormalities in the pygidial spines.

et al.'s (2007) supposition that Tsinaniidae is closely allied to Asaphidae. Rather, the protaspid morphology of *T. canens* is comparable to those of leiostegioid/illaenoid trilobites of the order Corynexochida in having a subhexagonal outline, a forwardly slightly expanding glabella, and a pair of anterior pits (see Chatterton 1980 for protaspides of *Nanillaenus mackenziensis*, *B. lenzi* and *Failleana calva*; Chatterton and Speyer 1997, fig. 171 for an unidentified illaenid protaspis; and Lee and Chatterton 2003 for the protaspis of *Leiostegium* sp. aff. *Leiostegium formosum*). In addition, the strongly downsloping trunk of an inverted-trapezoidal outline with an upturned lateral margin makes it discernable from the protaspides of the Cambrian ptychopariids (see Chatterton and Speyer 1997 for the descriptions of the ptychopariid protaspides). Especially the trunk with an upturned lateral margin is a feature visible only in some, if not all, protaspides of the order Corynexochida (see Lee and Chatterton 2003). Although the somewhat globular early stage protaspis of *T. canens* could be regarded to indicate a closer affinity with illaenid trilobites than with leiostegioids, the mature morphology of tsinaniids is discriminated from that of the Illaenidae in lacking the large rostral plate of inverse-triangular shape (see Whittington 1997; Bruthansová 2003): *T. canens* possessed a small triangular rostral plate behind a ventral median suture which disappeared later in development. Another key synapomorphy of illaenids is "the presence of an extra-axial cephalic muscle impression, the lunette (Fortey 1997, p. 299)." Albeit Fortey (1990, p. 565) mentioned that tsinaniids possess prominent muscle impressions lying outside the axial furrow which may be homologous to the lunette, neither *Tsinania* nor *Shergoldia* displays any structure comparable to the lunette. This implies that Tsinaniidae may not have been directly related to Illaenidae. Moreover, in the late-stage protaspis of *T. canens*, the anterior cranidial border is not recognizable or extremely narrow just as in that of *Leiostegium* sp. aff. *L. formosum*, whereas the late-stage protaspides of the Ordovician illaenids invariably possessed a somewhat well defined anterior cranidial border (see Chatterton 1980; Chatterton and Speyer 1997). This morphological similarity between the late-stage protaspides of *T. canens* and *Leiostegium* sp. aff. *L. formosum* suggests that Tsinaniidae was phylogenetically closer to leiostegioids than to illaenids.

Interestingly, the genal spines and the pygidial spines in the immature *T. canens* also support its close affinity to leiostegioids. In the Sino-Korean block, all the leiostegioid trilobite genera which occur in the Furongian strata older than the *Tsinania*-bearing horizon possess genal spines and paired pygidial spines: that is, *Kaolishania* Sun 1924, and *Mansuyia* Sun 1924 from the *Kaolishania* Zone (Zhang and Jell 1987; Qian 1994), and *Prochuangia* Kobayashi 1935 from the *Prochuangia* Zone (Kobayashi 1935; Qian 1994). It is noteworthy that *Mansuyia* immediately predates *T. canens* in occurrence and displays a more-or-less intermediate morphology between other older leiostegioids and *T. canens*: *Prochuangia* and *Kaolishania* bear well defined dorsal furrows, and *Mansuyia* shows somewhat effaced dorsal furrows, whereas *T. canens* has a completely effaced dorsal surface. In addition, *Mansuyia* has a slightly angulated anterior border just as *T. canens* does. Therefore, the genal and pygidial spines of immature specimens of *T. canens* are homologous to those

of the leiostegioids, supporting the assignment of Tsinaniidae within the Superfamily Leiostegioidea.

Polyphyletic origination of a ventral median suture

The ontogeny of *T. canens* reveals a close affinity with leiostegioids rather than with Asaphidae of the order Asaphida. Therefore, the superficial resemblance between tsinaniids and asaphids pointed out by Zhu et al. (2007) can be regarded as a result of convergent evolution. Zhu et al. (2007) argued that the small triangular rostral plate of *S. laevigata* represents an evolutionary prior stage to forming a ventral median suture. This study shows that the small triangular rostral plate would have disappeared during development resulting in a ventral median suture in *T. canens*.

The ventral median suture has been regarded as the key synapomorphy of the order Asaphida (Fortey and Chatterton 1988; Chatterton et al. 1994; Whittington 2003), although there have been doubts on the monophyletic origin of the ventral median suture (Whittington 2003, 2007). The ontogeny of *T. canens* for the first time demonstrates that the ventral median suture could have evolved polyphyletically. Especially, the formation of ventral median suture in *T. canens* via the reduction of the triangular rostral plate contrasts with the ventral median suture of the basal members of the current order Asaphidae which was claimed to be attained by the reduction of an inverted triangular rostellum (Chatterton et al. 1994), corroborating the polyphyletic evolution of the ventral median suture. The presence of a ventral median suture alone, therefore, will not be sufficient to guarantee an affinity with the current order Asaphida. It is suggested that the order Asaphida should be defined only by the presence of the asaphoid protaspis, and the basal members of the current order Asaphida, such as Anomocaridae, Dikelocephalinidae, Pterocephaliidae, and Parabolinoididae, which are not known to possess the asaphoid protaspis (Fortey and Chatterton 1988), should be excluded from the order Asaphida.

CONCLUSIONS

(1) *T. canens* had an adult-like late-stage protaspis. During the post-protaspid development, the dorsal furrows became effaced, a triangular rostral plate disappeared to form a ventral median suture, the genal spines regressed, and the pygidial spines abruptly disappeared.
(2) The degeneration of the genal and pygidial spines is a case of deleting transitory structures via programmed cell death. Especially, the radical removal of the pygidial spines during the holaspid phase is an unusual phenomenon in trilobites.
(3) Morphological changes during development such as the loss of genal and pygidial spines, modification of pleural tips, and effacement of dorsal furrows indicate that *T. canens* changed its life mode during ontogeny from benthic crawling to infaunal.
(4) The protaspid morphology and the presence of genal spines and pygidial spines in the immature morphology reveal that Tsinaniidae is closely tied to leiostegioids, discrediting the asaphid affinity suggested by Zhu et al. (2007). More importantly, *T. canens* developed a ventral median suture, which demonstrates that a ventral median suture could have evolved independently within a lineage other than the current order Asaphida. Regarding the ventral median suture as the key synapomorphy of the order Asaphida, therefore, should be reconsidered. It is suggested that the order Asaphida should be defined exclusively by the presence of the asaphoid protaspis.

Acknowledgments

We are grateful to Richard A. Fortey for the valuable comment on the early version of the manuscript. Constructive and insightful reviews by Nigel C. Hughes and John R. Paterson greatly improved the manuscript. Rudy Lerosey-Aubril, Thomas A. Hegna, and Paul S. Hong provided some literature. Financial support for this study has come from the Korea Research Foundation (Grant No. 2009-0078296). This article is a contribution to the BK 21 Project of the School of Earth and Environmental Sciences, Seoul National University.

REFERENCES

Bergström, J. 1973. Organization, life, and systematics of trilobites. *Fossils Strata* 2: 1–69.
Bookstein, F. L. 1991. *Morphometric Tools for Landmark Data*. Cambridge University Press, New York. 435pp.
Bruthansová, J. 2003. The trilobite Family Illaenidae Hawle et Corda, 1847 from the Ordovician of the Prague Basin (Czech Republic). *Trans. R. Soc. Edinb. Earth Sci.* 93: 167–190.
Chatterton, B. D. E. 1980. Ontogenetic studies of Middle Ordovician trilobites from the Esbataottine Formation, Mackenzie Mountains, Canada. *Palaeontogra. Abt. A* 171: 1–74.
Chatterton, B. D. E., and Ludvigsen, R. 1976. Silicified Middle Ordovician trilobites from the South Nahanni River area, District of Mackenzie, Canada. *Palaeontogra. Abt. A* 154: 1–106.
Chatterton, B. D. E., and Speyer, S. E. 1997. Ontogeny. In R. L. Kaesler (ed.). *Treatise on Invertebrate Paleontology, Part O, Arthropoda 1. Trilobita, Revised*. Geological Society of America and University of Kansas, Boulder, pp. 173–247.
Chatterton, B. D. E., Speyer, S. E., Hunt, A. S., and Fortey, R. A. 1994. Ontogeny and relationships of Trinucleoidea (Trilobita). *J. Paleontol.* 68: 523–540.
Choi, D. K., et al. 2004. Taebaek Group (Cambrian–Ordovician) in the Seokgaejae section, Taebaeksan Basin: a refined lower Paleozoic stratigraphy in Korea. *Geosci. J.* 8: 125–151.
Fallon, J. F., and Simandl, B. K. 1978. Evidence of a role for cell death in the disappearance of the embryonic human tail. *Am. J. Anat.* 152: 111–129.
Fortey, R. A. 1990. Ontogeny, hypostome attachment and trilobite classification. *Palaeontology* 33: 529–576.
Fortey, R. A. 1997. Classification. In R. L. Kaesler (ed.). *Treatise on Invertebrate Paleontology, Part O, Arthropoda 1. Trilobita, Revised.*

Geological Society of America and University of Kansas, Boulder, pp. 289–302.
Fortey, R. A. 2001. Trilobite systematics: the last 75 years. *J. Paleontol.* 75: 1141–1151.
Fortey, R. A., and Chatterton, B. D. E. 1988. Classification of the trilobite suborder Asaphina. *Palaeontology* 31: 165–222.
Fortey, R. A., and Owens, R. M. 1975. Proetida: a new order of trilobites. *Fossils Strata* 4: 227–239.
Hughes, N. C. 2007. The evolution of trilobite body patterning. *Annu. Rev. Earth Planet. Sci.* 35: 401–434.
Hughes, N. C., Minelli, A., and Fusco, G. 2006. The ontogeny of trilobite segmentation: a comparative approach. *Paleobiology* 32: 602–627.
Hupé, P. 1955. Classification des trilobites. *Ann. Paléontol.* 41: 91–325.
Jacobson, M. D., Weil, M., and Raff, M. C. 1997. Programmed cell death in animal development. *Cell* 88: 347–354.
Kobayashi, T. 1935. The Cambro–Ordovician formations and faunas of South Chosen. Paleontology, Part III, Cambrian faunas of South Chosen with a special study on the Cambrian trilobite genera and families. *J. Fac. Sci. Imperial Univ. Tokyo, Sect. II* 4: 49–344.
Kobayashi, T. 1952. On *Mansuyia* and the Tsinaniidae. *Trans. Proc. Palaeont. Soc. Jpn., N. S.* 5: 145–154.
Kwon, Y. K., Chough, S. K., Choi, D. K., and Lee, D. J. 2006. Sequence stratigraphy of the Taebaek Group (Cambrian–Ordovician), mideast Korea. *Sediment. Geol.* 192: 19–55.
Kimura, K. I., and Truman, J. W. 1990. Postmetamorphic cell death in the nervous and muscular systems of *Drosophila melanogaster*. *J. Neurosci.* 10: 403–411.
Lee, D.-C., and Chatterton, B. D. E. 2003. Protaspides of *Leiostegium* and their implications for membership of the Order Corynexochida. *Palaeontology* 46: 431–445.
Milligan, C. E., and Schwartz, L. M. 1997. Programmed cell death during animal development. *Br. Med. Bull.* 52: 570–590.
Moczek, A. P. 2006. Pupal remodeling and the development and evolution of sexual dimorphism in horned beetles. *Am. Nat.* 168: 711–729.
Moczek, A. P., Cruickshank, T. E., and Shelby, A. 2006. When ontogeny reveals what phylogeny hides: gain and loss of horns during development and evolution of horned beetles. *Evolution* 60: 2329–2341.
Nakajima, K., Fujimoto, K., and Yaoita, Y. 2005. Programmed cell death during amphibian metamorphosis. *Semin. Cell Dev. Biol.* 16: 271–280.
Qian, Y. 1994. Trilobites from the middle Upper Cambrian (Changshan Stage) of north and northeast China. *Palaeontol. Sin., New Ser. B* 30: 1–176, 34 pls (in Chinese with English summary).
Sapunar, D., Vilović, K., England, M., and Saraga-Babić, M. 2001. Morphological diversity of dying cells during regression of the human tail. *Ann. Anat.* 183: 217–222.
Schwartz, L. M. 1992. Insect muscle as a model for programmed cell death. *J. Neurobiol.* 23: 1312–1326.
Shergold, J. H. 1975. Late cambrian and early ordovician trilobites from the Burke River Structural Belt, Western Queensland, Australia. *Bureau Miner Resour. Geol. Geophys. Bull.* 153: 1–251.
Shergold, J. H. 1991. Late Cambrian and early Ordovician trilobite faunas and biostratigraphy of the Pacoota Sandstone, Amadeus Basin, central Australia. *Bureau Mineral Resour. Geol. Geophys. Bull.* 237: 15–76.
Sohn, J. W., and Choi, D. K. 2007. Furongian trilobites from the *Asioptychaspis* and *Quadraticephalus* zones of the Hwajeol Formation, Taebaeksan Basin, Korea. *Geosci. J.* 11: 297–314.
Stitt, J. H. 1976. Functional morphology and life habits of the late Cambrian trilobite *Stenopilus pronus* Raymond. *J. Paleontol.* 50: 561–576.
Sun, Y. C. 1924. Contribution to the Cambrian faunas of North China. *Palaeontol. Sin. (B)* 1: 1–109.
Tata, J. R. 1966. Requirement for RNA and protein synthesis for induced regression of the tadpole tail in organ culture. *Dev. Biol.* 13: 77–94.
Vaux, D., and Korsmeyer, S. J. 1999. Cell death in development. *Cell* 96: 245–254.
Walcott, C. D. 1905. Cambrian faunas of China. *Proc. U.S. Nat. Mus.* 29: 1–106.
Westrop, S. R. 1983. The life habits of the Ordovician illaenine trilobite *Bumastoides*. *Lethaia* 16: 15–24.
Whittington, H. B. 1957. The ontogeny of trilobites. *Biol. Rev.* 32: 421–469.
Whittington, H. B. 1997. Illaenidae (Trilobita): morphology of thorax, classification, and mode of life. *J. Paleontol.* 71: 878–896.
Whittington, H. B. 2003. The upper Cambrian trilobites *Plethopeltis* and *Leiocoryphe*: morphology, paedomorphism, classification. *J. Paleontol.* 77: 698–705.
Whittington, H. B. 2007. Reflections on the classification of the Trilobita. In D. G. Mikulic and E. Landing (eds.). *Fabulous Fossils—300 Years of Worldwide Research on Trilobites. N.Y. State Mus. Bull.* New York State Museum, Albany, NY, 507. pp. 225–230.
Zelditch, M. L., Swiderski, D. L., Sheet, H. D., and Fink, W. L. 2004. *Geometric Morphometrics for Biologists: a Primer*. Elsevier Academic Press, San Diego, CA. 443pp.
Zhang, W. T., and Jell, P. A. 1987. *Cambrian Trilobites of North China: Chinese trilobites housed in the Smithsonian Institution*. Science Press, Beijing, 459pp.
Zhu, X.-J., Hughes, N. C., and Peng, S.-C. 2007. On a new species of *Shergoldia* Zhang & Jell, 1987 (Trilobita), the family Tsinaniidae and the order Asaphida. *Mem. Assoc. Australas. Palaeontol.* 34: 243–253.